Journal of Pest Science
https://doi.org/10.1007/s10340-024-01831-9

ORIGINAL PAPER

Exploring multigene families of odorant binding proteins and cytochrome P450 monooxygenases in the stink bug pest complex through comparative transcriptomics

Andrea Belén Dulbecco[1] · Débora Elizabeth Moriconi[1] · Fernanda Cingolani[2] · Eliana Nieves[2] · Luis Diambra[3] · Nicolás Pedrini[1]

Received: 12 April 2024 / Revised: 9 August 2024 / Accepted: 19 August 2024

Abstract

The stink bugs *Edessa meditabunda*, *Piezodorus guildinii*, and *Diceraeus furcatus* (Hemiptera: Pentatomidae) are major pests in the Argentinean core area of soybean production. A detailed molecular genetics comprehension of how these insects perceive odorants and respond to semiochemicals and how they detoxify chemical pesticides and plant compounds are essential to improve their management strategies. We first assembled and compared the transcriptomes from *E. meditabunda*, *P. guildinii*, and *D. furcatus*. Regarding sequence similarity, *P. guildinii* and *D. furcatus* are closer to each other than *E. meditabunda.* Then, we characterized the multigene families of odorant binding proteins (OBPs) and cytochrome P450 monooxygenases (CYP). A total of 29, 38, and 39 unigenes encoding for OBP were obtained in *E. meditabunda*, *P. guildinii*, and *D. furcatus*, respectively, divided into classical OBPs and plus-C OBPs. A total of 72, 63, and 76 unigenes encoding for CYP were found in *E. meditabunda*, *P. guildinii*, and *D. furcatus*, respectively, which were further classified into 24 families and 47 subfamilies. On the other hand, we performed for the first time RNA interference in vivo by dsRNA injection in *E. meditabunda*, suggesting that this molecular tool can be exploited in future physiological and functional studies in this species.

Keywords Chemoreception · CYP · Insecticide detoxification · Metabolic resistance · OBPs · RNAseq

Introduction

The stink bug complex (Hemiptera: Pentatomidae) includes insects known by its ability to release a bad odor when disturbed or when crushed. Most stink bugs are phytophagous insects considered major pests of crops worldwide, especially in the Neotropical Region, where the largest

Communicated by Swevers Luc.

Andrea Belén Dulbecco and Débora Elizabeth Moriconi shares first authorship.

✉ Nicolás Pedrini
npedrini@med.unlp.edu.ar

Andrea Belén Dulbecco
adulbecco@med.unlp.edu.ar

Débora Elizabeth Moriconi
dmoriconi@med.unlp.edu.ar

Fernanda Cingolani
fernandacingolani@cepave.edu.ar

Eliana Nieves
elianánieves@cepave.edu.ar

Luis Diambra
ldiambra@gmail.com

[1] Instituto de Investigaciones Bioquímicas de La Plata (INIBIOLP), CCT La Plata Consejo Nacional de Investigaciones Científicas y Técnicas (CONICET) - Universidad Nacional de La Plata (UNLP), Calles 60 y 120, 1900 La Plata, Argentina

[2] Centro de Estudios Parasitológicos y de Vectores (CEPAVE) CCT La Plata Consejo Nacional de Investigaciones Científicas y Técnicas (CONICET), Universidad Nacional de La Plata (UNLP), Boulevard 120 E/ 60 y 64, 1900 La Plata, Argentina

[3] Centro Regional de Estudios Genómicos (CREG), Facultad de Ciencias Exactas, Universidad Nacional de La Plata (UNLP), CONICET, Boulevard 120 1459, 1900 La Plata, Argentina

Published online: 03 September 2024

total production of basic agricultural commodities such as soybean, maize, cotton, rice, and wheat are concentrated (Panizzi et al. 2022). Argentina is the world's fourth largest soybean producer, cultivating 13,809,328 hectares in 2021, which represents approximately 12.5% of the global soybean cultivated area (source: http://www.fao.org/faostat/en/#data). The more frequent species within the stink bug complex found in the Argentinean core area of soybean production (provinces of Buenos Aires, Santa Fe, and Córdoba) are the southern green stink bug *Nezara viridula* (Linnaeus), the brown-winged stink bug *Edessa meditabunda* (Fabricius), the red-banded stink bug *Piezodorus guildinii* (Westwood), and the green-belly stink bug *Diceraeus furcatus* (Fabricius) (Balbi et al. 2023; Cingolani et al. 2014; Jacobi et al. 2022).

Chemical communication is essential for stink bugs fitness since they locate their food by sensing plant volatile cues (Jacobi et al. 2022). Also, stink bugs secrete and perceive chemical signals (semiochemicals) to facilitate a complex interplay either among themselves (pheromones) or with other insects (allelochemicals) (Moraes et al. 2008). Insect detection of a wide range of volatiles is mostly mediated by the odorant binding proteins (OBPs) and chemosensory proteins (CSPs), which play an important role in both uptake and transport of the chemical signal to the odorant receptors (ORs), ionotropic receptors (IRs), and gustatory receptors (GRs), which are mainly expressed in taste-sensing neurons. In addition, the sensory neuron membrane proteins (SNMPs) are suggested to play an important role in odorant detection (Vogt 2003). From all these genes, the OBPs is the more abundant complex. It is encoded by a multigene family described within 10 different insect orders. Although OBPs show little sequence similarity between species, the conservation of six cysteines (Cys) is always maintained (Zhou et al. 2004). Based on the number of conserved Cys, OBPs are classified into different subfamilies: classical OBPs (six Cys), plus-C (more than six Cys, including at least three additional cysteines, along with a conserved proline), and minus-C (less than six Cys) (Zhou et al. 2004; Pelosi et al. 2006). A study on related soybean stink bugs from Brazil has shown that each species holds between seven and twenty-five OBPs, with most of them belonging to the classical OBPs subfamily (Farias et al. 2015).

Current control strategies of stink bugs are heavily based on chemical pesticides spraying, mainly pyrethroids but also organophosphates and neonicotinoids (Sosa-Gómez et al. 2020). However, their massive and recurrent use is concerning due to the well-known negative impact to human health and the environment, as same as the growing levels of tolerance and/or resistance reported within stink bug populations (Sosa-Gómez et al. 2020; Du et al. 2024). Monitoring of insecticide resistance but also understanding the mechanisms involved are very important for a successful chemical control of insects (Amichot et al. 2023). One of the mechanisms best described is the metabolic resistance, i.e., a greater capacity to detoxify insecticides due to an increase in either gene expression or enzyme activity related to xenobiotics detoxification (Haddi et al. 2023). The cytochrome P450 monooxygenases, which are encoded by CYP genes, constitute the primary enzyme superfamily associated with insect metabolic resistance (Dermauw et al. 2020). In herbivorous insects, cytochrome P450s have also been proposed to mediate in insect adaptation on host plants, catalyzing the monooxygenation of plant secondary metabolites and/or allelochemicals that are detrimental to the bug fitness (Després et al. 2007; Feyereisen 2011; Li et al. 2007; Xu et al. 2005). All CYP genes described in insects were classified into clans CYP2, CYP3, CYP4 and the mitochondrial CYP clan; both CYP3 and CYP4 clans have been associated with metabolic resistance (Dermauw et al. 2020; Dulbecco et al. 2021) and CYP3 clan has also been linked with herbivore adaptation on plant hosts (Feyereisen 2011).

A comprehensive understanding of the molecular genetics of these processes, i.e., how stink bugs perceive odorants and respond to semiochemicals, as well as how they detoxify chemical pesticides and plant compounds, are essential to improve their management strategies. There is little genetic information available for the stink bug complex; the whole genome has been released for *Halyomorpha halys* (Stål) (Sparks et al. 2020), *P. guildinii* (Saha et al. 2022), and *Euschistus heros* (Fabricius) (Singh et al. 2023). However, there are several transcriptomic studies in *H. halys* (Sparks et al. 2014), *N. viridula* (Lavore et al. 2018; Riga et al. 2020), *E. heros*, *Chinavia ubica* (Rolston), *Diceraeus melacanthus* (Dallas) (Cagliari et al. 2020; Farias et al. 2015), and *P. guildinii* (Schvartzman et al. 2022) that provide some clues to understand these processes.

In this study, we assembled and compared the transcriptomes from the three more abundant stink bugs in soybean crops from Buenos Aires province, Argentina, i.e., *E. meditabunda*, *P. guildinii*, and *D. furcatus*. By using both gene ontology (GO) and kyoto encyclopedia of genes and genomes (KEGG) databases, we specifically addressed OBPs and CYPs, two of the most abundant multigene superfamilies in insects, which are known to be involved in volatile detection and insecticide resistance, respectively (Sánchez-Gracia et al. 2009; Feyereisen 2011). On the other hand, we performed for the first time in *E. meditabunda* an RNA interference approach by dsRNA injection showing that this species is susceptible to RNAi and thus confirmed that this approach might be exploited in future physiological and functional studies on this stink bug.

Materials and methods

Insects rearing

Colonies of the stink bugs *E. meditabunda*, *P. guildinii*, and *D. furcatus* were established from field-collected insects at the Julio Hirschhörn Experimental Station, Faculty of Agricultural Sciences and Forestry, National University of La Plata (345924.32S, 58018.51W; 27 m.s.n.m.). Insects were fed *ad libitum* with green bean pods (*Phaseolus vulgaris*) and maintained at 24 ± 1 ºC, 70 ± 10 % relative humidity, and a photoperiod of 14:10 (L:D) h.

Sample preparation for transcriptomes sequencing

Total RNA was extracted from whole bodies of ten first instar nymphs of each species (2–3 days after hatching) using TRIzol Reagent (Invitrogen, Carlsbad, CA, USA), following manufacturer's instructions. Total RNA was quantified on a Nanodrop 2000c spectrophotometer (Thermo Scientific, Waltham, MA, USA), and its quality was assessed with 1% (w/v) agarose gel electrophoresis. Immediately after extraction, 2 µg of total RNA of each sample was lyophilized and shipped to Novogene (Davis, CA, USA) for sequencing on an Illumina NovaSeq platform. The construction of cDNA libraries was performed from RNA samples by using NEBNext Ultra II RNA kit with the PolyA enrichment method, for Illumina paired end (PE) sequencing following the Illumina protocol. The sequencing strategy was PE150, which gives 150 bp read from each end to make a 300-bp sequenced fragment.

Transcriptomes assembly

The raw reads obtained from each assembly contained reads contaminated with adapters and low-quality reads. To prevent them from affecting the downstream analysis, the raw reads was filtered by an in-house script based on FASTP (0.23.1) as follows: (i) removing reads with adapter contamination, (ii) removing reads when low-quality nucleotides ($Q < 5$) constitute more than 50% of the read, (iii) removing reads with a percentage greater than 10% of uncertain nucleotides (N). The clean sequences of each sample were then used for the transcriptome reconstruction. *P. guildinii* has a genome assembled (Saha et al. 2022), but no reference genomes are known for the other two species. Despite the potential for a mapping transcriptome assembly to achieve better quality than a *de novo* assembly, a *de novo* transcriptome assembly was performed for all three species to avoid potential biases that could arise from comparing transcriptomes analyzed using different methodologies. Trinity software (Grabherr et al. 2011) was used for *de novo* transcriptome assembly. The workflow of Trinity comprises three main steps: (i) inchworm that constructs a k-mer dictionary from all sequenced reads (we use a k-mer ≥ 31 bases long), (ii) chrysalis that clusters minimally overlapping assembled contigs into sets of connected components, and constructs complete de Bruijn graphs for each component, and (iii) butterfly that reconstructs plausible, full-length, linear transcripts by reconciling the individual de Bruijn graphs generated by Chrysalis with the original paired end reads. The final assembled transcriptomes, one for each species, were recorded in FASTA format (X_Trinity.fasta, where "X" means the species name) and deposited at https://zenodo.org/records/10433299). A BioProject was established with the raw reads, which have been deposited in the sequence reads archive (SRA) at NCBI under accession number PRJNA1034521.

The assembled transcript sequences were clustered by using Corset (Davidson and Oshlack 2014) which works by clustering contigs based on shared reads. Corset also filters out contigs with a low number of mapped reads (less than 10 reads by default). The longest transcripts of each cluster were selected as unigenes, recorded in FASTA format as unigene (X_Unigene.fasta), and deposited at https://zenodo.org/records/10433299). The transcript abundance was estimated by mapping the pair-reads of each sample to the corresponding reference genome. The Corset-filtered reconstructed transcriptome of each species was used as a reference. The software used to do the alignment was RSEM (Li and Dewel 2011). The quality of each assembly was evaluated with Benchmarking Universal Single-Copy Orthologs (BUSCO) and by the percentage of reconstructed coding transcripts with BLAST match against Swiss-Prot database.

Unigene datasets were compared among species using CD-HIT-EST-2D (Li and Godzik 2006) to identify the sequences in one dataset that exhibit similarity to the other dataset above a specified threshold. In this comparison, identity thresholds of 60% and 90% were employed. For each species, those unigene sequences whose predicted ORFs had a BLAST match with a protein in the NR or Swiss-Prot databases were selected (with an e-value threshold 1e-5). In addition, unigenes with no hits in BLAST were analyzed with TransDecoder to predict their coding regions and to determine their sequence direction. Coding region of the Unigenes identified by BLAST (X_Unigene_CD_blast.fasta), predicted by Transcoder (X_Unigene_CD_transdec.fa), and the peptide product (X_Unigene_pep_blast.fasta) were also deposited at https://zenodo.org/records/10433299).

Gene annotation

To achieve a comprehensive functional annotation of the three assembled transcriptomes, unigene sequences were contrasted against seven annotation databases. An align search of the unigenes was performed against NR by using Diamond (Buchfink et al. 2014) with an e-value threshold of 1e-5 and keeping with top-10 alignment results. Through HMMER program (v 3.2), unigenes were scanned against the curated protein families (PFAM) profile database with hmmscan and an e-value threshold of 0.01. Further, Blast2GO (Götz et al. 2008) was used to select the gene ontology (GO) terms, which were associated with each unigene from the GO pool obtained from the two previous annotation steps and assign them to the unigene sequences with e-value threshold 1e-6. Finally, KEGG ortholog annotation was assigned to the unigene sequences by using the KEGG automatic annotation server (KAAS) with an e-value threshold 1e-5 and functional annotation of genes by comparisons against the manually curated KEGG GENES database. This procedure was performed for the three species, and their results (deposited at https://zenodo.org/records/10433299) constitute a transcriptional resource for further studies (X_annotation.tsv).

Identification of odorant binding protein (OBP) and cytochrome P450 monooxygenase (CYP) genes

To find all putative genes of interest, the genome-wide annotation made in the previous step was used. Unigenes with GO terms of odorant binding (GO:0005549) were selected from GO annotation profiles. Additionally, the sequences associated with two PFAM IDs (PF01395 and PF00067, which correspond to OBP and P450 genes, respectively) were selected from PFAM annotation profiles. For OBP characterization, the number of conserved cysteines (Cys motif) was used as a signature, and then named as classical OBPs (six Cys), plus-C (more than six Cys), and minus-C (less than six Cys) (Pelosi et al. 2006). For CYP genes, all the sequences with high homology found in the three assembled transcriptomes were sent to Dr. David Nelson (University of Tennessee, Memphis, TN, USA) and officially named by the P450 Nomenclature Committee. Transcripts shorter than 130 aa (OBPs) and 250 aa (CYPs) were ignored to avoid overestimation.

Multiple sequence alignment and phylogenetic analysis

Multiple sequence alignments were performed using Clustal Omega (http://www.clustal.org/omega) (Madeira et al. 2022). OBPs alignments were analyzed using Jalview (Waterhouse et al. 2009), and signal peptides were predicted using SignalP 6.0 (Teufel et al. 2022). Phylogenetic trees were constructed with the amino acid sequences of the OBPs (after removal of putative signal peptides) and CYPs mentioned above, along with the corresponding sequences from the related stink bugs *H. halys* (Paula et al. 2016; Bansal and Michel 2018) and *N. viridula* (Wu et al. 2019; Denecke et al. 2020). The trees were constructed based on the approximately maximum likelihood approach with 1000 bootstrap replications using IQ-tree v 2.11.3.0 (Nguyen et al. 2014). The best-fit amino acid substitution model estimated by IQ-tree for each protein family and chosen according to Bayesian information criterion (BIC) was Q.insect+I+R3 in Mitochondrial CYP clan, Q.plant+R4 for CYP2 clan, Q.plant+F+I+R6 for CYP3 clan and Q.plant+F+R6 for CYP4 clan.

Synthesis and purification of dsRNA

Edessa meditabunda transcriptome was screened for vATPAase A nucleotide sequence using as a query *H. halys* protein sequence XM_014417043.2. Double-stranded RNA (dsRNA) was synthesized using the MEGAscript RNAi kit (Ambion, Austin, TX, USA) following manufacturer's recommendations. DNA template, which served for dsRNA synthesis, was amplified by PCR using primers containing the T7 RNA polymerase promoter at their 5' end. Primers were designed using the GeneRunner software. The PCRs were done using the Platinum Taq DNA Polymerase (Invitrogen, Carlsbad, CA, USA) in total volumes of 50 µl, according to manufacturer's instructions. Temperature program for PCRs was an initial denaturing cycle at 94 °C for 2 min, followed by 35 cycles at 94 °C for 30 s, 55 °C for 30 s, and 72 °C for 1 min. DNA and dsRNA concentrations were measured on a Nanodrop 2000c spectrophotometer, and their quality and size verified on a 1% (w/v) agarose gel electrophoresis.

Silencing by RNAi and mortality assay

Adults of *E. meditabunda* (randomly males and females) were intra-abdominal (ventral) injected with dsRNA. Each insect was injected with 2 µl of either dsRNA solution at 0.5 µg/µl for dsvATPase (42 insects) or dsRNA for the control gene provided with the silencing kit (control group) (42 insects). Forty-eight hours later, 12 injected insects of each group were selected randomly, and the gene silencing efficiency was checked out by RT-qPCR as detailed below. The remaining insects (30 for each treatment) were used to check daily mortalities. The control dsRNA consists in a fragment of *Xenopus* elongation factor 1α gene. The relative transcript expression of *E. meditabunda* vATPAse A was measured in midgut samples by RT-qPCR on an AriaMx Real-Time PCR instrument (Agilent Technologies, Santa Clara, CA, USA)

using the iQ SYBR-Green Supermix (Bio-Rad, Hercules, CA, USA). RT-qPCR reactions contained 5 µl Sybr-Green supermix, 4 µl cDNA diluted 10-fold, 0.4 µl of each primer (200 nM), and Milli-Q water in a 10 µl total volume. Temperature program for RT-qPCR was: one initial denaturation cycle at 95 °C for 3 min, followed by 40 cycles at 95 °C for 15 s, and 60 °C for 60 s. A post-amplification melting curve analysis was carried out to check for unspecific product formation, under the following temperature program: 95 °C for 30 s, 65 °C for 30 s, and then an increase in temperature to 95 °C for 30 s where total SYBR-Green fluorescence was measured every 0.5 °C. Ubiquitine and 18S were used as housekeeping genes for normalization of gene expression. The stability of the reference genes was tested using the GeNorm algorithm (Vandesompele et al. 2002). No template and no reverse transcriptase controls were analyzed to detect potential primer dimer formation and contamination with genomic DNA, respectively. Primer efficiencies were determined using fivefold dilution series (1:5 down to 1:3125) from pooled cDNA to generate standard curves for each primer pair. Standard curves were obtained to evaluate the PCR efficiency of each primer pair used, and the comparative Ct (ΔΔCt) method was employed for relative quantification (Pfaffl 2001). Two technical replicates of each of the three independent biological samples were run. To analyze the efficiency in vATPaseA silencing, the NRQ model was applied, consisting of the conversion of quantification cycle values (Cq) into normalized relative quantities (NRQs), the adjustment for differences in PCR efficiency between the amplicons, and the normalization with reference genes (Hellemans et al. 2007).

Mortalities were recorded every 24 h after dsRNA injections for a period of 10 days. Survival curves were estimated using the nonparametric Kaplan–Meier method followed by a log-rank test to compare the survival between groups ($\alpha = 0.05$). Graph Pad Prism 5.01 software (GraphPad Software, San Diego, CA, USA) was used for statistical analyses.

RESULTS

Comparative transcriptomes of E. meditabunda, *P. guildinii*, and *D. furcatus*: characterization and completeness analysis

The number of raw reads obtained from each transcriptome was 46,015,783; 54,855,665; and 49,215,385 for *E. meditabunda*, *P. guildinii*, and *D. furcatus*, respectively. The sequences are subject to sequencing errors and base quality varies depending on sample types; thus, the error rate distribution along reads for the three samples is depicted in Supplementary Figure S1. After applying the filtering process, the number of clean reads obtained was 45,019,409; 53,569,947; and 47,900,239 for *E. meditabunda*, *P. guildinii*, and *D. furcatus*, respectively (Suppl. Table S1). Most of the data were composed of clean reads and the Q20 scores were > 96% in the three samples. Supplementary Figure S2 shows the length distribution of both transcripts and unigenes for each sample. A total of 42,070; 32,587; and 36,808 unigenes with an N50 length of 1736, 1906, and 1737 bp for *E. meditabunda*, *P. guildinii*, and *D. furcatus* transcriptomes, respectively, were assembled using Trinity. Completeness of the transcriptomes evaluated by BUSCO showed that 91.3%, 95.7%, and 97.0% of unigenes were identified in *E. meditabunda, P. guildinii,* and *D. furcatus*, respectively; while the number of unigenes with a BLASTx match (e-value threshold 1e-5) obtained against the Swiss-Prot database was 11,483 (27.3%); 10,928 (33.5%), and 12,474 (33.9%) for *E. meditabunda, P. guildinii,* and *D. furcatus*, respectively. These completeness metrics indicated that the assembled transcriptomes have sufficient coverage for further gene family characterization. To carry out the gene annotation of transcriptome assemblies, a protein alignment technique against the non-redundant protein sequences (NCBI, NR Database) using Diamond software (Buchfink et al. 2014) was employed. The alignments were computed using the unigene sequences of other insect species. Figure 1 shows that most of the newly reported sequences in this study possess an ortholog in *H. halys*, commonly known as the brown marmorated stink bug, which is the first pentatomid species to have its genome sequenced (Sparks et al. 2020). To putatively identify the function of unigenes, the sequences were aligned against seven databases to decipher gene function: NR (NCBI non-redundant protein sequences), NT (NCBI nucleotide sequences), PFAM (Protein family), KOG/COG: COG (Cluster of Orthologous Groups of proteins) and KOG (euKaryotic Orthologous Groups), Swiss-Prot, KEGG, and GO. Approximately 50% of the unigenes were annotated in at least one database. The results summary is shown in Supplementary Table S2. The transcript abundance of each species was estimated from the Corset-filtered reconstructed transcriptomes. The obtained gene-FPKM (fragments per kilobase per million mapped fragments) values for each insect are listed in Supplementary Table S3, while the brief mapping statistic is displayed in Supplementary Table S4.

Sequence identity

To identify the sequences in one species that exhibit similarity to the other species, the unigenes whose predicted ORF and BLAST matched with a protein in NR and Swiss-Prot databases were selected. These encompassed 12,780; 11,917; and 13,111 sequences from *E. meditabunda, P. guildinii* and *D. furcatus*, respectively. Figure 2 illustrates the comparisons of these unigene datasets among the three species, taken pairwise, at the nucleotide level using

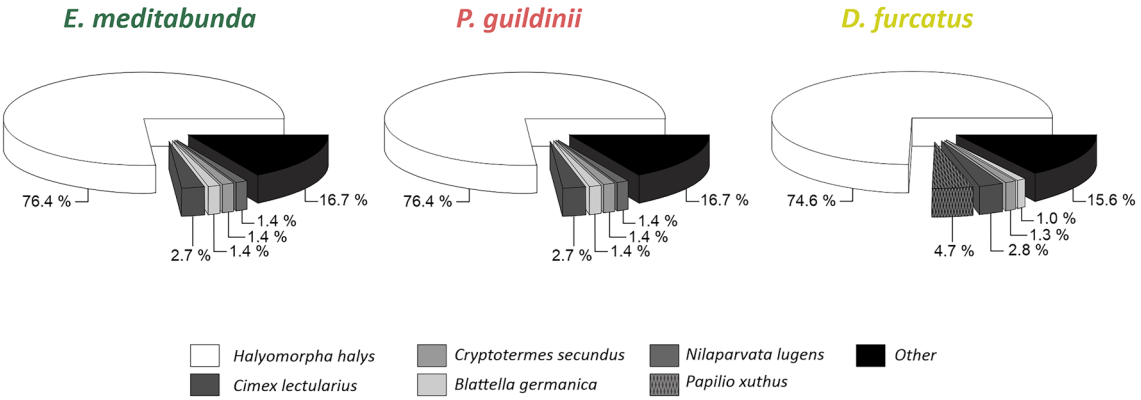

Fig. 1 Classification of unigenes. Similarity of the unigenes from *Edessa meditabunda, Piezodorus guildinii* and *Diceraeus furcatus* transcriptomes with sequences of other insect genera (bitscore > 50) is expressed as percentage of coincidence using the NR protein database from NCBI (BLASTx)

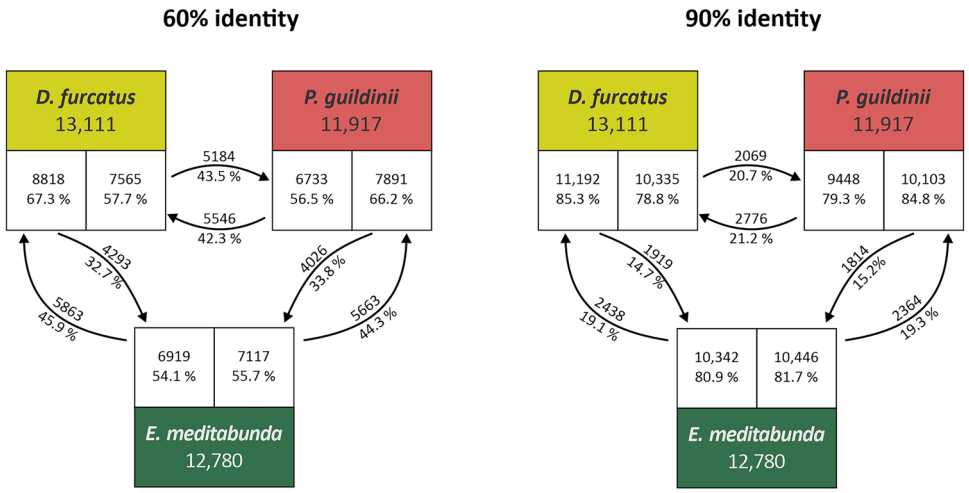

Fig. 2 Sequence similarity between *Edessa meditabunda*, *Piezodorus guildinii* and *Diceraeus furcatus* unigene datasets. Identity thresholds of 60% and 90% were set using CD-HIT-EST-2D. For each species, only those unigene sequences which predicted ORF having a BLAST match with a protein in NR and Swiss-Prot databases were used. Colored rectangles represent the total sequences for *E. meditabunda* (green), *P. guildinii* (red), and *D. furcatus* (yellow) used in the analysis. The numbers in the arrows indicate the quantity and percentage of sequences that are not shared between species taken pairwise; the number inside the squares indicates the quantity and percentage of sequences that are shared between species taken pairwise

CD-HIT-EST-2D (Li and Godzik 2006). At an identity level of 60%, it was observed that 42.3% out of the 131,111 sequences identified in *D. furcatus*, were also found in *P. guildinii*, whereas only 32.7% were present in *E. meditabunda*. When comparing *P. guildinii* to *D. furcatus*, similar sequences (around 43.5%) were found between species, whereas the comparison of *P. guildinii* to *E. meditabunda* revealed only 33.8% of the 11,917 unigenes in *P. guildinii* have a similar unigene in *E. meditabunda*. Similar patterns were observed when conducting these comparisons at a sequence identity of 90% (Fig. 2). These findings suggest that the transcript sequences of *D. furcatus* and *P. guildinii* exhibit a higher degree of similarity to each other compared to *E. meditabunda,* which exhibited lower values.

Gene Ontology (GO) annotation

A total of 11,887; 10,833; and 12,750 predicted GO terms were obtained for *E. meditabunda*, *P. guildinii* and *D. furcatus*, respectively, and then categorized into three groups: cellular components, biological processes, and molecular function (Suppl. Fig. S3). The most dominant GO terms within categories were the same for the three species, i.e., cellular process for cellular components, cellular anatomical

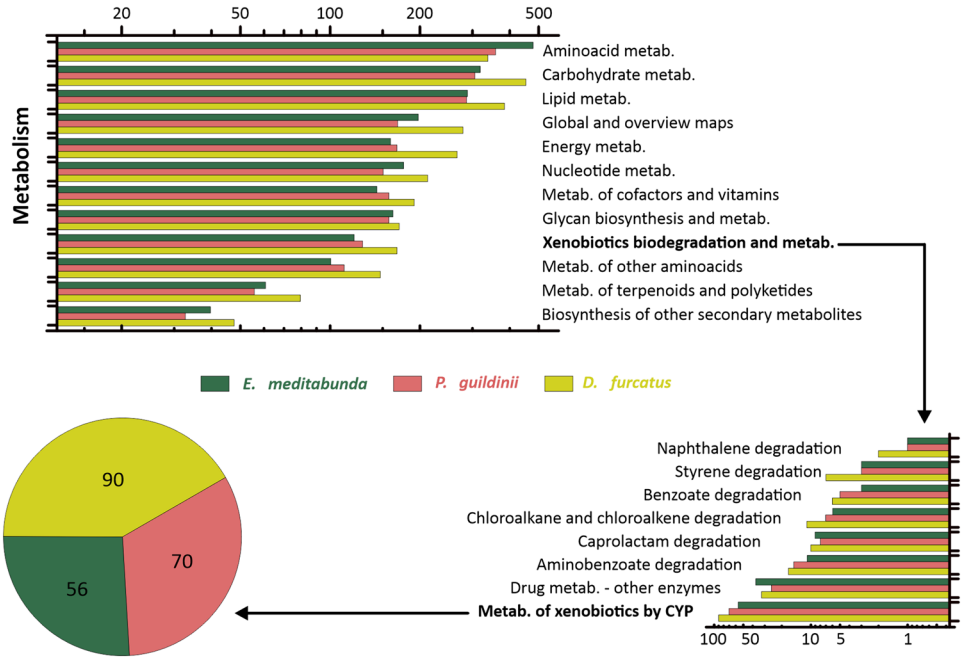

Fig. 3 Comparison of KEGG pathway map corresponding to unigenes categorized into the "Metabolism" group between *Edessa meditabunda* (green), *Piezodorus guildinii* (red) and *Diceraeus furcatus* (yellow). The x-axis indicates the number of unigenes annotated under each pathway detailed at the right side. "Xenobiotics biodegradation and metabolism" was further categorized into 8 specific groups. The circle represents the number of P450 genes that are putatively involved in "Metabolism of xenobiotics by CYP" in *E. meditabunda* (green), *P. guildinii* (red), and *D. furcatus* (yellow)

entity for biological processes, and binding for molecular function (Suppl. Fig. S3).

KEGG pathways analyses

The prediction of unigenes into metabolic pathways was performed by querying the KEGG database. A total of 7359, 7016, and 8034 unigenes were obtained for *E. meditabunda, P. guildinii* and *D. furcatus*, respectively. They were categorized into five groups, i.e., cellular processes, environmental information processing, genetic information processing, metabolism, and organismal systems (Suppl. Fig. S4). Figure 3 shows that "metabolism" was further classified into 12 KEGG pathways, among them, "xenobiotic biodegradation and metabolism" (including 121, 129 and 168 unigenes for *E. meditabunda*, *P. guildinii*, and *D. furcatus*, respectively). This group is formed by other 8 subgroups, being cytochrome P450 monooxygenases the most abundant. The total CYP genes found within this subgroup were 56, 70, and 90 in *E. meditabunda*, *P. guildinii*, and *D. furcatus*, respectively (Fig. 3).

Identification and characterization of OBP and CYP transcripts

Genome-wide annotations from the three transcriptomes were used to find the genes that putatively encode for OBPs and CYPs. From GO annotation profiles, the unigenes with GO terms corresponding to odorant binding activity (GO:0005549) were selected. Additionally, the PFAM profiles were addressed for annotation of OBP (PFAM ID: PF01395) and cytochrome P450 (PFAM ID: PF00067). These sequences were then manually curated, and those with low homology with their corresponding gene families were discarded. The CYP sequences were officially named and classified into the corresponding CYP clans (Suppl. Table S5). A total of 29, 38, and 39 unigenes encoding for

Table 1 Total number of unigenes putatively encoding for odorant binding protein (OBP) obtained from de novo assembled transcriptomes of *Edessa meditabunda, Piezodorus guildinii,* and *Diceraeus furcatus*

Multigene family	*Edessa meditabunda*	*Piezodorus guildinii*	*Diceraeus furcatus*
Classical	25	31	36
Plus-C	4	7	3
Total OBP	29	38	39

Table 2 Total number of unigenes putatively encoding for Cytochrome P450 monooxigenases (CYP) obtained from de novo assembled transcriptomes of *Edessa meditabunda*, *Piezodorus guildinii*, and *Diceraeus furcatus*

Multigene family	*Edessa meditabunda*	*Piezodorus guildinii*	*Diceraeus furcatus*
Mito clan	4	4	4
CYP2 clan	4	4	5
CYP3 clan	37	33	39
CYP4 clan	27	22	28
Total CYP	72	63	76

OBP (Table 1), and a total of 72, 63, and 76 CYP unigenes were found in *E. meditabunda*, *P. guildinii*, and *D. furcatus*, respectively (Table 2).

Odorant binding proteins

Classical OBPs: From the total OBP genes detected in each species, *E. meditabunda* contained 25 genes, *P. guildinii* 31 genes, and *D. furcatus* 36 genes belonging to the classical OBP family, representing 86%, 82%, and 92% of total OBPs, respectively. Alignments of these sequences showed that all of them exhibited the typical six-conserved cysteines arrangement (Cys motif) (Fig. S5). Classical OBPs are grouped within a distinct cluster in the phylogenetic tree (Fig. 4).

Plus-C OBPs: They represented 14% of total OBP genes in *E. meditabunda*, 18% in *P. guildinii*, and 7% in *D. furcatus*. Figure S5 describes the sequences alignment of these sequences. They all maintained the six Cys pattern, the conserved proline located immediately after the sixth Cys, and the three additional Cys residues. They also exhibita "CC" pattern at the N terminus. (Fig. S5). Phylogenetic analysis revealed a distinctive cluster exclusively formed by plus-C OBPs (Fig. 4).

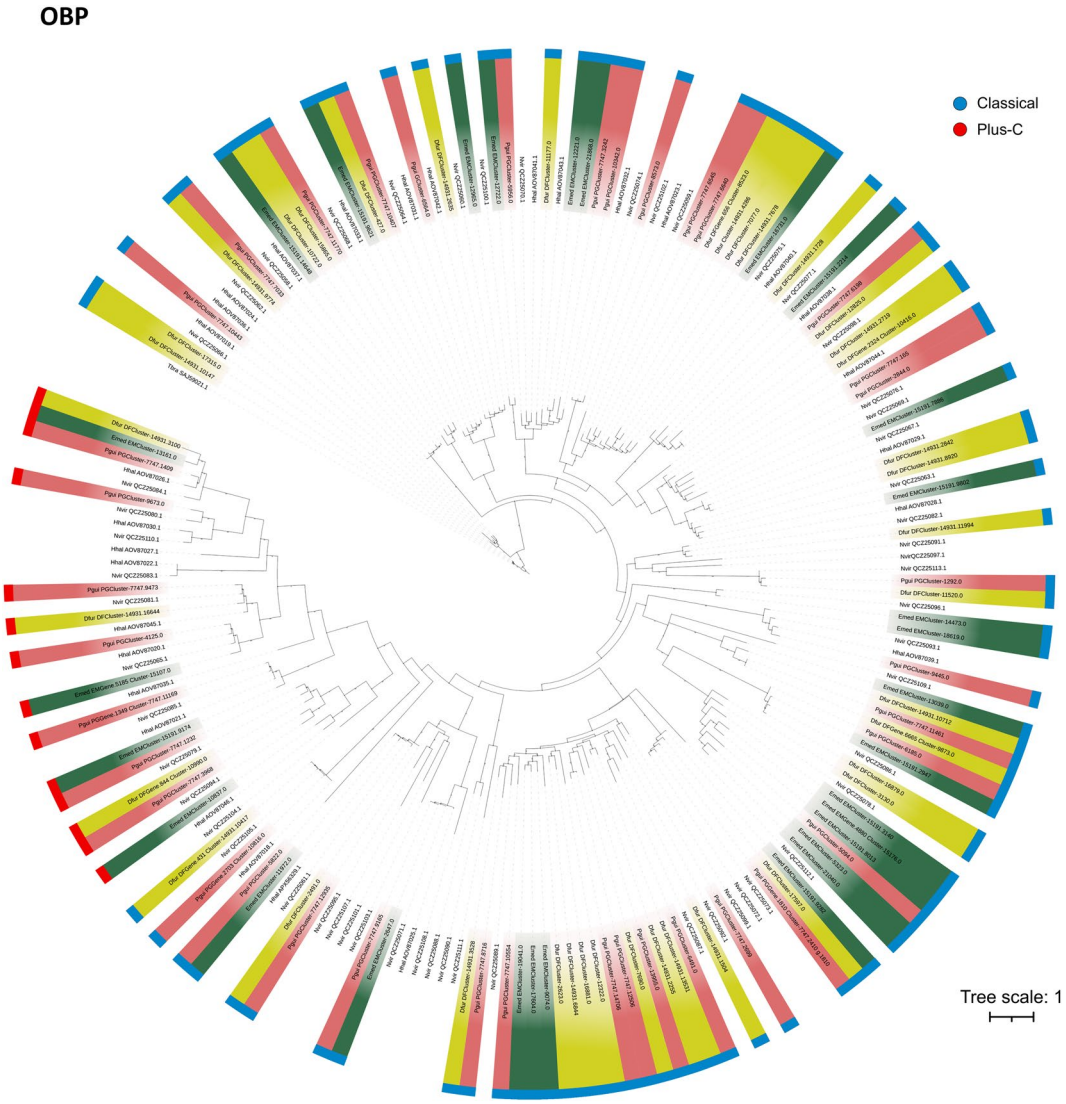

Fig. 4 Phylogenetic trees of deduced peptide sequences of putative OBPs (after removal of putative signal peptides) from *Edessa meditabunda, Piezodorus guildinii* and *Diceraeus furcatus*. The OBP families (classical and plus-C) are detailed on the right side and represented by different colors in the tree outline. All nodes have significant bootstrap support based on 1000 replicates. The bootstrap values only above 80% are shown next to branches. The OBP sequences that correspond to *E. meditabunda*, *P. guildinii* and *D. furcatus* are highlighted in green, red, and yellow, respectively. An OBP gene from *Triatoma brasiliensis* was used as an outgroup (SAJ59021.1). The complete sequences used for the trees are detailed in Supplementary Table S6

Cytochrome P450 monooxygenases

The P450s encoded by the four CYP clans were further classified into 24 families and 47 subfamilies, as is detailed in Supplementary Table S5. The evolutionary history of each clan across these three pentatomids, and the related *H. halys* and *N. viridula*, were inferred using the maximum likelihood approach (Fig. 5). The CYP2 clan contains five genes in *E. meditabunda* and their orthologs in *D. furcatus* (CYP18A1, CYP303A1, CYP305L1, CYP306A1 and CYP307B1), and four genes in *P. guildinii* (CYP18A1, CYP303A1, CYP306A1 and CYP307B1). The mitochondrial clan is represented by families CYP301, CYP302, CYP314, and CYP315. It contains four genes both in *E. meditabunda* and *P guildinii,* and five genes in *D. furcatus*. *Edessa meditabunda* has one member of each subfamily (CYP301A1, CYP302A1, CYP314A1 and CYP315A1) while *P. guildinii* and *D. furcatus* has two members of CYP301 subfamily (CYP301A1 and B1) and one member of CYP314 (CYP314A1) and CYP315 (CYP315A1). The fifth member in *D. furcatus* corresponded to the CYP302 subfamily (CYP302A1) (Supplementary Table S5).

Both CYP3 and CYP4 clans have a greater number of genes than clans 2 and mitochondrial clans, possibly due to gene expansions in concordance with similar data from other insects (Feyereisen 2011). The CYP3 clan contained

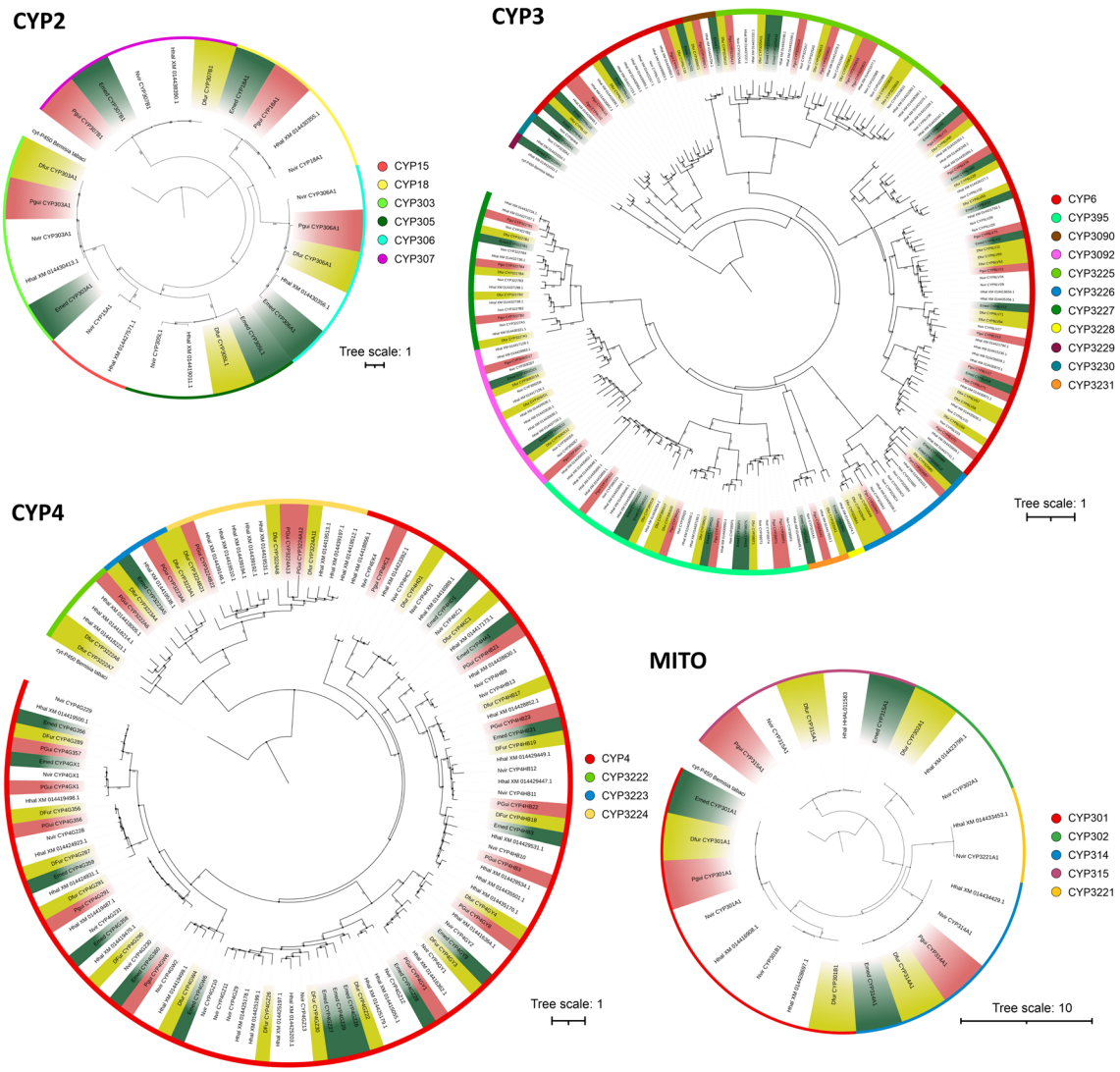

Fig. 5 Phylogenetic trees of CYP clans (Mito, CYP2, CYP3, CYP4) from *Edessa meditabunda, Piezodorus guildinii*, *Diceraeus furcatus, Nezara viridula*, and *Halyomorpha halys*. The CYP families are detailed on the right side and represented by different colors in the outline of each tree. All nodes have significant bootstrap support based on 1000 replicates. The bootstrap values only above 80% are shown next to branches. The P450 sequences that correspond to *E. meditabunda, P. guildinii and D. furcatus* are highlighted in green, red, and yellow, respectively. A CYP gene from *Bemisia tabaci* was used as an outgroup (AEK21835.1). The complete sequences used for the trees are detailed in Supplementary Table S7

38 members in *E. meditabunda*, 33 in *P. guildinii*, and 39 in *D. furcatus*. The main expanded family was represented by CYP6, which comprised subfamilies CYP6HK, CYP6LT, CYP6LU, and CYP6LV. Family CYP6 includes 13 members in both *E. meditabunda* and *P. guildinii*, and 17 members in *D. furcatus*, containing at least one member of each subfamily in each species, except for CYP6HK that was not found in *P. guildinii*. The second larger subfamily in CYP3 clan was CYP395, which included subfamilies CYP395P, CYP395Q, CYP395R, CYP395S, and CYP395T, with 8 genes in *E. meditabunda,* 5 genes in *P. guildinii*, and 6 genes in *D. furcatus*. The CYP395R subfamily was only found in *P. guildinii.* The remaining CYP3 clan members are genes from families CYP3225 to 3231, CYP3090, and CYP3092 (Suppl. Table S5). Subfamilies CYP3228, 3229 and 3230 were only represented in *E. meditabunda,* and subfamily CYP3090 and CYP3092 were not found in *D. furcatus* (Suppl. Table S5).

The CYP4 clan comprised 27 members in *E. meditabunda*, 22 members in *P. guildinii,* and 28 members in *D. furcatus*. The phylogenetic analysis showed that this clan was segregated in two main clades, one of them corresponding to the family CYP4 and the other one with members of families CYP3222 to 3224, which were mixed-up between species. The CYP4 family was the largest from the CYP4 clan, with 25 members in *E. meditabunda*, 14 in *P. guildinii*, and 18 in *D. furcatus*. It is represented by subfamilies CYP4KC, CYP4EK, CYP4HA, CYP4HB, CYP4HD, CYP4G, CYP4GW, CYP4GX, CYP4GY and CYP4GZ. The CYP4KC subfamily was only present in *P. guildinii* (CYP4KC1), while subfamilies CYP4EK and CYP4HA were only found in *E. meditabunda* (CYP4EK6 and CYP4HA1). Both *E. meditabunda* and *D. furcatus* have one member of CYP4HD subfamily (CYP4HD1) that was not found in *P. guildinii*. Regarding CYP4GW and CYP4GX, the three species contained 1 member each. *Edessa meditabunda* has one CYP4GY member (CYP4GY9), and 12 members of CYP4GZ subfamily (CYP4GZ26 to CYP4GZ29 plus 8 gene fragments). *Piezodorus guildinii* has 2 members of CYP4GY subfamily (CYP4GY1 and GY8), and two fragments corresponding to CYP4GZ subfamily. *Diceraeus furcatus* also has 2 members of CYP4GY subfamily (CYP4GY3 and GY4) and 3 members of CYP4GZ subfamily (CYP4GZ22, GZ26 and GZ30). Regarding families CYP3222 to 3224, each species has at least one gene representing each family, except for *E. meditabunda* to whom no expression of CYP3222 gene family was found (Suppl. Table S5).

dsRNA injection in Edessa meditabunda

To assess the efficiency of RNAi technique in *E. meditabunda*, the effect of dsRNA targeting dsvATPase A by injection in adults was addressed. We decided to test dsvATPase A because it has been a model gene for silencing in several species from the stink bug complex, showing good phenotypes to evaluate from a functional point of view (Mogilicherla et al. 2018; Castellanos et al. 2019; Riga et al. 2020; Cagliari et al. 2020; Gurusamy et al. 2021; Schvartzman et al. 2022). A significant reduction in its expression ($97.2 \pm 1.5\%$, $P < 0.001$) was found in comparison with control insects at 48 h post-treatment (Fig. 6A). The silencing effect on survival of insects was measured by the median survival time, which was 5 days for ATPase-silenced insects, being significantly different between groups ($\chi 2 = 9{,}934$, df = 1, $P = 0.0016$) (Fig. 6B). Primers used are detailed in Table S8.

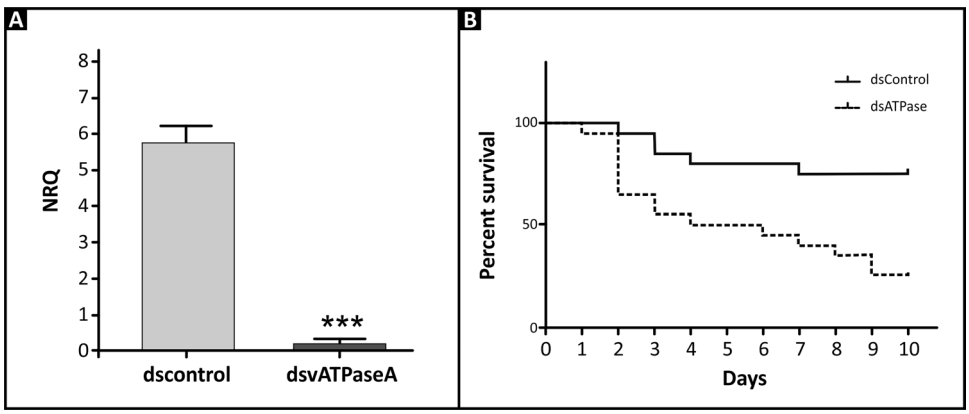

Fig. 6 RNA interference targeting vATPase A in *Edessa meditabunda*. **A** Relative expression of vATPase transcript in dsvATPase- or dsControl-injected insect. The normalized relative quantity (NRQ) was estimated using 18S and ubiquitine as reference genes. Error bars represent standard error of the means of 3 biological replicates. Asterisk indicates significant difference between treatments determined by a Student's *t*-test (***, $P < 0.001$). **B** Mortality bioassay of dsvATPase- and dsControl-injected insects over time. The cumulative mortality for 10 days is plotted for each insect sample

Discussion

Stink bugs cause losses in crop production, deformities in fruits, and affect the quality and viability of seeds. They also produce indirect damage by acting as vectors of pathogenic microorganisms causing diseases to the plants. These pests attack a wide variety of plants such as lettuce, tomato, eggplant, strawberry, quinoa, sunflower, corn, wheat, cotton, and soybean, among other crops. A recent review on the pest status of pentatomids noted that *N. viridula* and *P. guildinii* were the most significant pest species until their decline in the last decade. Conversely, *E. heros*, *D. melacanthus*, and *D. furcatus*, previously considered minor pests, emerged as major pests in the 2010s. Additionally, while *E. meditabunda* never reached high populations, the species has shown an increasing trend in abundance over the last two decades (Panizzi et al. 2022). Despite the economic losses that these stink bugs represent annually, little genetic information is available. Recent transcriptomic studies have focused on xenobiotic metabolism (Denecke et al. 2020) and neuropeptide precursors (Lavore et al. 2018) in *N. viridula*, siRNA machinery in *E. heros* (Cagliari et al. 2020) and in *P. guildinii* (Schvartzman et al. 2022), and analysis of chemosensory genes in the antennae of *Arma chinensis* (Fallou) (Hemiptera: Pentatomidae) (Wu et al. 2020). The genomic resources generated in the current study significantly advance research on fundamental aspects of stink bug biology. The quality of assembled transcriptomes was suitable for comprehensive analysis and characterization of transcribed multigene families. Specifically, the transcript sequences obtained enabled us the mining of putative OBPs and CYPs of these important species.

The number of transcript sequences shared among the three stink bug species studied indicates that *D. furcatus* and *P. guildinii* are more closely related to each other than to *E. meditabunda*. This relationship may be linked to certain biological characteristics, as the first two species share similar feeding habits, primarily using reproductive structures of plants (fruits and seeds) as their main food source (Grazia et al. 2008; Rider et al. 2017). In contrast, *E. meditabunda* predominantly feeds on vegetative structures (leaflet and stem) (Lucini and Panizzi 2017), which generally contain high water and low nutrient levels compared to seeds (Taiz and Zeiger 2004). Furthermore, *D. furcatus* and *P. guildinii* exhibit less polyphagy than *E. meditabunda* (Panizzi 1997). Consequently, some of the genes shared by *D. furcatus* and *P. guildinii* may play a role in various aspects of the feeding process, including the ability to locate suitable plants through olfaction, digestion and nutrients acquisition, detoxification of secondary metabolites from plant defenses against herbivory, etc. (Dallagnol and Cônsoli 2024). It is well known that several allelochemicals and secondary metabolites are present in plant tissues, some of which possess toxic and/or repellent properties to insects (Panizzi 1987). These compounds include lectins, flavonoids, alkaloids, steroids, and phenolic acids, as well as anti-nutritional factors such as trypsin inhibitors, anti-vitamins, and phytic acid (Panizzi 1987). The repertoire of enzymes and binding proteins expressed by each stink bug species may enable them to manage these compounds, thereby influencing the range of plants they can utilize as food and the impact their feeding may have on crops. For instance, Lucini et al. (2017) demonstrated that *P. guildinii* is the most damaging among the several species of stink bug pests of soybean, due to the maceration of seed tissues caused by the action of its saliva (Depieri and Panizzi 2011). The arrangement of transcripts within each species resulting from our analysis is supported by the phylogeny of the group, established based on morphological and molecular characteristics. Indeed, *D. furcatus* and *P. guildinii* are classified within the same subfamily (Pentatominae), whereas *E. meditabunda* is assigned to a different subfamily (Edessinae) (Ferrari et al. 2015). These phylogenetic relationships among species also reflect common patterns of physiological, behavioral, and ecological characteristics, which are highly relevant for designing control strategies against the different stink bug insect pests.

In most animals, perception of the environment is mainly guided by chemical signals, which modulate several traits such as food and mate finding, mating, defensive and assembly behaviors, the acquisition of gut symbionts, among others. Some of these traits can be targeted for pest management strategies (Pal et al. 2023). The dynamic process of signal detection involves transport of chemical signals to odorant receptors by soluble odorant binding proteins (OBPs), which constitute the initial stage in olfactory recognition. However, detailed information on olfactory detection and the molecular mechanisms through which OBPs participate in the transport of several of the chemical cues used by insects remains limited. Antony et al. (2018) performed expression analysis of all OBPs of the palm pest *Rhynchophorus ferrugineus* (Olivier) (Coleoptera: Curculionidae) and selected antenna-specific and highly expressed OBPs for silencing through RNA interference. They found that silencing a specific OBP responsible for pheromone binding, significantly disrupted pheromone communication. This disruption may affect the process of mating of the pest, contributing to its control. RNAi assays also confirmed that an OBP from the red flour beetle *Tribolium castaneum* (Herbst) (Coleoptera: Tenebrionidae) is required for both reproduction and defense against phytochemicals (Gao et al. 2023).

In this study, we identified a total of 29, 38, and 39 OBPs in *E. meditabunda*, *P. guildinii*, and *D. furcatus*,

respectively; some more than those reported in the related stink bugs *E. heros* (23 OBPs) and *C. ubica* (25 OBPs), and much more than *D. melacanthus* (9 OBPs) (Farias et al. 2015). The similar number of OBPs we found in *P. guildinii* and *D. furcatus* reinforce the hypothesis of genetic difference between both species with *E. meditabunda*. Indeed, the total number of OBP in stink bugs is higher than those from other Hemiptera in the Miridae, Aphididae and Delphacidae families, suggesting that stink bugs might retain the same biological function to bind same ligands perceived or produced by insects within the stink bug complex (Farias et al. 2015). The predominan of OBPs was similar in both studies, with mostly classical OBPs and fewer Plus-C OBPs. In our current study, we did not identify any minus-C OBP, whereas Farias et al. (2015) found one minus-C among the three other stink bugs studied.

Insect cytochrome P450 monooxygenases are a superfamily of enzymes involved in the degradation of xenobiotics, both from diet and the environment, but also participate in key metabolic processes such as pheromones degradation and signaling molecules biosynthesis (Dermauw et al. 2020). In winged insects (Neoptera), the genes encoding for P450s (CYP) are classified into four clans, i.e., CYP2, CYP3, CYP4 and mitochondrial clans (Dermauw et al. 2020). Comparing with the CYPomes from other pentatomid species, the number of CYP found in this study was similar to those described in *N. viridula* (85) but lower than those in *H. halys* (132) (Bansal and Michel 2018; Volonté et al. 2022). Mitochondrial clan genes tend to be highly conserved among insect species, due to their essential roles in the life cycle, for example, encoding Halloween genes that are involved in ecdysteroid synthesis (Feyereisen 2011). Thus, the number of mitochondrial clan genes was similar between species of the stink bug complex, i.e., 8 in *H. halys* (Volonté et al. 2022), 6 in *N. viridula* (Volonté et al. 2022), 4 in *E. meditabunda*, 4 in *P. guildinii*, and 5 in *D. furcatus*. This clan is represented by 5 CYP families (CYP301, CYP302, CYP314, CYP315 and CYP3221), with at least one member of each family in each specie, except for family CYP3221 that was absent in the transcriptomes evaluated in this study.

Regarding CYP2 clan, it is represented by 6 families (CYP15, CYP18, CYP303, CYP305, CYP306 and CYP307) in *H. halys*, with one member in each family (Volonté et al. 2022). Family CYP15 was not represented in any species analyzed in the present study, nor was family CYP305 in *P. guildinii*. In insects, both mitochondrial and CYP2 clans are associated with core functions in development and physiology, whereas CYP3 and CYP4 clans are linked with environmental interactions. Thus, CYP3 and CYP4 clans are always much larger than mitochondrial and CYP2 clans in insect genomes, because of species- or lineage-specific expansions that allowed their diversification and specialization (Feyereisen 2011).

The number of genes belonging to CYP3 clan described in this study is like those found for *N. viridula* (41) (Feyereisen 2011) but much lower than those for *H. halys* (75) (Bansal and Michel 2018). The number of P450 genes in insect genomes is highly variable but, in general, polyphagous herbivores possess a significantly larger repertoire of P450 genes than oligophagous, presumably to cope with diverse and unpredictable host challenges (Rane et al. 2019). As members of CYP3 clan are usually implicated in herbivore adaptation on plant hosts (Feyereisen 2011), the discrepancy in the number of CYP3 genes between *H. halys* and the other pentatomids might be due to their diet's habits. The main expanded family found in this study was CYP6, with 7 gene fragments belonging to subfamily CYP6LV. This subfamily is apparently exclusive of pentatomids, the same as families CYP3225 to CYP3231 (Volonté et al. 2022). Although the gene fragments from subfamily CYP6LV described in this study were not included in the phylogenetic tree because of their small size, they support the hypothesis of gene expansion.

In pentatomids, the CYP4 clan was represented by families CYP4 and CYP3222 to CYP3224. Volonté et al. (2022) reported 32 members of CYP4 clan in *N. viridula* and 43 members in *H. halys*, whereas 22 to 28 genes were described for each of the three species in this study. Regarding the family CYP4, members from subfamilies CYP4HA, CYP4HB, CYP4HC, CYP4HD, CYP4EK, CYP4KC, CYP4G, CYP4GW, CYP4GX, CYP4GY, and CYP4GZ were described. Both *H. halys* and *N. viridula* have one gene in the subfamilies CYP4HA, CYP4GHC, and CYP4HD, and the CYP4HB subfamily contains five to eight members (Riga et al. 2020; Volonté et al. 2022). From the three species analyzed in our study, only *E. meditabunda* have a member in the subfamily CYP4EK and CYP4HA but lack CYP4HC. Both *D. furcatus* and *P. guildinii* have one member each of CYP4HC. Subfamily CYP4KC is only present in *D. furcatus* with one member. Subfamily CYP4HB contains three or four members in the species analyzed in this study. Regarding the CYP4G subfamily, both *H. halys* and *N. viridula* show two clusters of genes, one with six tandem duplicated genes and another with two. From the six-gene cluster, four of them are CYP4G (named as CYP4G156 to CYP4G159 in *H. halys,* and CYP4G228 to CYP4G231 in *N. viridula*) (Riga et al. 2020; Volonté et al. 2022), whereas the other two genes were named into new subfamilies (CYP4GW1 and CYP4GX1) owing to their divergence from the original CYP4G sequence (Feyereisen 2020). The harlequin bug *Murgantia histrionica* (Hahn) (Hemiptera: Pentatomidae), and *N. viridula* have also the corresponding CYP4GW and CYP4GX orthologs (Denecke et al. 2020; Volonté et al. 2022), and both *H. halys* and *N. viridula* have two members of CYP4GY subfamily (4GY1 and 4GY2), and several members of CYP4GZ subfamily (Denecke et al. 2020; Volonté

et al. 2022). Feyereisen (2020) proposed that CYP4G genes from the order Hemiptera evolved from a common ancestor of a CYP4G15 gene, leading not just to several gene gains and losses, but also to greater sequence divergence within some subfamilies (e.g., CYP4GW to CYP4GZ) that are exclusive of stink bugs. The three species analyzed in this study contain one gene in the subfamilies CYP4GW and CYP4GX, and the CYP4GY subfamily contains 1 member in *E. meditabunda* and two members in *P. guildinii* and *D. furcatus*. Regarding CYP4GZ, *P. guildinii* contains 2 members, *D. furcatus* contains 3 members, and *E. meditabunda* contains 12 members. Interestingly, the 10 gene fragments are identified in this study (8 in *E. meditabunda* and 2 in *P. guildinii*) belonging to the subfamily CYP4GZ also supporting the hypothesis of gene expansion.

An important aspect concerning the chemical control of the stink bug pests complex is the differential susceptibility of each species to insecticides. In this sense, it has been demonstrated that *P. guildinii* exhibits four- to eightfold less susceptible to pyrethroids and two- to eightfold lower susceptibility to organophosphates compared to *N. viridula* (Temple et al. 2013). A recent study conducted in soybean crops in Mississippi indicated that *P. guildinii* showed reduced susceptibility to neonicotinoids compared to other stink bugs collected over the past two seasons, a phenomenon correlated with elevated esterase and cytochrome P450 activity (Du et al. 2024). Although the efficiency of pesticides against stink bugs was largely studied, and it is well known that cytochrome P450s are related to detoxification, the mechanisms involved in each species susceptibility to chemical pesticides has not received much attention. Our findings in relation to CYP genes of the species studied provide important knowledge that contributes to disentangle the potential of chemical control as part of a set of strategies that may be implemented in the frame of an integrated pest management.

RNA interference (RNAi) is a very useful technique to assess gene functions. One promising application of RNAi involves systematically knocking down genes to identify novel targets for pest control. Genes that cause lethality when knocked-down (KD-lethal genes), such as small molecules, proteins, or even dsRNA is applied in several Coleopteran species such as *T. castaneum* (Knorr et al. 2018) and *Diabrotica virgifera* Krysan & Smith (Coleoptera: Chrysomelidae) (Hu et al. 2016). In the stink bug complex, several studies confirmed the effectiveness of the RNAi machinery targeting a dsRNA of the *V-ATPase-A* gene (dsvATPase A). Gene expression was significantly reduced in treated animals, and the mortality rate was increased in *E. heros* (Cagliari et al. 2020; Castellanos et al. 2019), *H. halys* (Mogilicherla et al. 2018), *N. viridula* (Riga et al. 2020; Gurusamy et al. 2021) and *P. guildinii* (Schvartzman et al. 2022) after topically injection with dsvATPase A. In the present study, we evaluated *in vivo* whether RNAi was functional in adult *E. meditabunda* after dsRNA injection targeting vATPase. Our results showed an increased mortality effect and a significant reduction in the relative expression of vATPase at 48 h after injection. These results demonstrate for the first time that *E. meditabunda* is susceptible to RNAi, with a significant mortality effect. Thus, RNAi is an interesting approach for future studies and the development of control strategies in this species, as well as in the other species from stink bug complexes already described.

In conclusion, the results of this study provide valuable molecular information that expand the knowledge in the biology of three of the main important species of phytophagous stink bugs, responsible for severe damage to economically important crops in the Neotropical region, mostly soybean in the reproductive stage.

Supporting information

The transcriptome sequence and annotations presented in this study can be found in the online repository Zenodo (https://zenodo.org/records/10433299). The raw sequence dataset is available at the NCBI (https:// PRJNA1034521).

Author contributions

A.B.D, D.E.M, and N.P. conceived and designed the experiments. A.B.D, D.E.M, F.C., E.N., L.D. performed the experiments. A.B.D, D.E.M, L.D., and N.P. analyzed the data. N.P. wrote the manuscript. All authors reviewed the manuscript.

Supplementary Information The online version contains supplementary material available at https://doi.org/10.1007/s10340-024-01831-9.

Acknowledgements This study was funded by the Agencia Nacional de Promoción Científica y Tecnológica from Argentina, grants PICT 2020 01322 to A.B.D. and PICT 2019 02974 to N.P. The authors thank Mario Ramos for figures preparation, Guillermo Benítez for phylogenetic analysis, and Dr. David Nelson for CYP naming.

Funding The authors have no relevant financial or non-financial interests to disclose.

Data availability The transcriptome sequence and annotations presented in this study can be found in the online repository Zenodo (https://zenodo.org/records/10433299). The raw sequence dataset is available at the NCBI (https:// PRJNA1034521).

Declarations

Conflict of interest The authors declare no conflict of interests.

References

Amichot M, Brun-Barale A, Haddi K, Nauen R, Guedes RNC, Tarès S (2023) Current knowledge on the origin of insecticide resistance mechanisms: the tip of the iceberg? Entomol Gen 43:501–503

Balbi EI, Flores FM, Arneodo JD (2023) First genetic analysis of *Euschistus heros* F. (Hemiptera: Pentatomidae) from Argentina and its relative abundance in a newly invaded soybean region. Phytoparasitica 51:379–384

Bansal R, Michel A (2018) Expansion of cytochrome P450 and cathepsin genes in the generalist herbivore brown marmorated stink bug. BMC Genomics 19:1–14

Antony B, Johny J, Aldosary SA (2018) Silencing the odorant binding protein RferOBP1768 reduces the strong preference of Palm Weevil for the major aggregation pheromone compound ferrugineol. Front Physiol 9:252

Buchfink B, Xie C, Huson DH (2014) Fast and sensitive protein alignment using DIAMOND. Nat Methods 12:59–60. https://doi.org/10.1038/nmeth.3176

Cagliari D, Dias NP, dos Santos EA, Rickes LN, Kremer FS, Farias JR et al (2020) First transcriptome of the Neotropical pest *Euschistus heros* (Hemiptera: Pentatomidae) with dissection of its siRNA machinery. Sci Rep 10:1–16

Castellanos NL, Smagghe G, Sharma R, Oliveira EE, Christiaens O (2019) Liposome encapsulation and EDTA formulation of dsRNA targeting essential genes increase oral RNAi-caused mortality in the Neotropical stink bug *Euschistus heros*. Pest Manag Sci 75:537–548

Cingolani M, Greco MN, Liljesthröm GG (2014) Egg parasitism of *Piezodorus guildinii* and *Nezara viridula* (Hemiptera: Pentatomidae) in soybean, alfalfa and red clover. Rev Fac Cienc Agrar 46:15–27

Dallagnol LC, and Cônsoli FL (2024) Evolutionary and phylogenetic insights from the mitochondrial genomic analysis of *Diceraeus melacanthus* and *D. furcatus* (Hemiptera: Pentatomidae). Sci. Rep. 14: 12861. https://doi.org/10.1038/s41598-024-63584-w

Davidson NM, Oshlack A (2014) Corset: enabling differential gene expression analysis for de novo assembled transcriptomes. Genome Biol 15:7

Denecke S, Ioannidis P, Buer B, Ilias A, Douris V, Topalis P et al (2020) A transcriptomic and proteomic atlas of expression in the *Nezara viridula* (Heteroptera: Pentatomidae) midgut suggests the compartmentalization of xenobiotic metabolism and nutrient digestion. BMC Genomics 21:1–15

Depieri R, Panizzi A (2011) Ecology, behavior and bionomics duration of feeding and superficial and in-depth damage to soybean seed by selected species of stink bugs (Heteroptera: Pentatomidae). Neotrop Entomol 40:197–203

Dermauw W, Van Leeuwen T, Feyereisen R (2020) Diversity and evolution of the P450 family in arthropods. Insect Biochem Mol Biol 127:103490

Després L, David JP, Gallet C (2007) The evolutionary ecology of insect resistance to plant chemicals. TREE 22:298–307

Du Y, Scheibener S, Zhu YC, Allen KC, Reddy GVP (2024) Insecticide susceptibilities and enzyme activities of four stink bug populations in Mississippi, USA. Insects 15:265. https://doi.org/10.3390/insects15040265

Dulbecco AB, Moriconi DE, Pedrini N (2021) Knockdown of CYP4PR1, a cytochrome P450 gene highly expressed in the integument tissue of *Triatoma infestans*, increases susceptibility to deltamethrin in pyrethroid-resistant insects. Pestic Biochem Physiol 173:104781. https://doi.org/10.1016/j.pestbp.2021.104781

Farias LR, Schimmelpfeng PHC, Togawa RC, Costa MMC, Grynberg P, Martins NF et al (2015) Transcriptome-based identification of highly similar odorant-binding proteins among neotropical stink bugs and their egg parasitoid. PLoS ONE 10:1–23

Ferrari A, Barão KR, Bianchi FM, Campos LA, Grazia J (2015) Classification and biogeography of neotropical true bugs. True Bugs (Heteroptera) of the Neotropics. Springer, Netherlands, pp 57–87. https://doi.org/10.1007/978-94-017-9861-7_3

Feyereisen R (2011) Insect CYP Genes and P450 Enzymes. In: Molecular I (ed) Lawrence I Gilbert. Academic Press, Biology and Biochemistry, pp 236–316

Feyereisen R (2020) Origin and evolution of the CYP4G subfamily in insects, cytochrome P450 enzymes involved in cuticular hydrocarbon synthesis. Mol Phylogenet Evol 143:106695

Gao S, Huo Z, Guo M, Zhang K, Zhang Y, Wang X et al (2023) Contact toxicity of eucalyptol and RNA sequencing of *Tribolium castaneum* after exposure to eucalyptol. Entomol Res 53:226–237

Gonella E, Orrù B, Marasco R, Daffonchio D, Alma A (2020) Disruption of host-symbiont associations for the symbiotic control and management of Pentatomid agricultural pests—a Review. Front Microbiol 11:547031

Götz S, García-Gómez JM, Terol J, Williams TD, NagarajNueda SHMJ et al (2008) High-throughput functional annotation and data mining with the Blast2GO suite. Nucleic Acids Res 36:3420–3435

Grabherr MG, Haas BJ, Yassour M, Levin JZ, Thompson DA, Amit I et al (2011) Full-length transcriptome assembly from RNA-Seq data without a reference genome. Nat Biotechnol 29:644–652

Grazia J, Schuh RT, Wheeler WC (2008) Phylogenetic relationships of family groups in Pentatomoidea based on morphology and DNA sequences (Insecta: Heteroptera). Cladistics 24(6):932–976

Gurusamy D, Howell JL, Chereddy SCR, Mogilicherla K, Palli SR (2021) Improving RNA interference in the southern green stink bug. Nezara Viridula J Pest Sci 94:1461–1472

Haddi K, Nauen R, Benelli G, Guedes RNC (2023) Global perspectives on insecticide resistance in agriculture and public health. Entomol Gen 43:495–500

Hellemans J, Mortier G, De Paepe A, Speleman F, Vandesompele J (2007) qBase relative quantification framework and software for management and automated analysis of real-time quantitative PCR data. Genome Biol 8:R19

Hu X, Richtman NM, Zhao JZ, Duncan KE, Niu X, Procyk LA et al (2016) Discovery of midgut genes for the RNA interference control of corn rootworm. Sci Rep 6:30542

Jacobi VG, Fernández PC, Zavala JA (2022) The stink bug Dichelops furcatus: a new pest of corn that emerges from soybean stubble. Pest Manag Sci 78:2113–2120

Knorr E, Fishilevich E, Tenbusch L, Frey MLF, Rangasamy M, Billion A et al (2018) Gene silencing in *Tribolium castaneum* as a tool for the targeted identification of candidate RNAi targets in crop pests. Sci Rep 8:2061

Lavore A, Perez-Gianmarco L, Esponda-Behrens N, Palacio V, Catalano M, Rivera-Pomar, et al (2018) Nezara viridula (Hemiptera: Pentatomidae) transcriptomic analysis and neuropeptidomics. Sci Rep 8:17244

Li W, Godzik A (2006) Cd-hit: a fast program for clustering and comparing large sets of protein or nucleotide sequences. Bioinformatics 22:1658–1659

Li X, Schuler MA, Berenbaum MR (2007) Molecular mechanisms of metabolic resistance to synthetic and natural xenobiotics. Annu Rev Entomol 52:231–253

Li B, Dewey CN (2011) RSEM: accurate transcript quantification from RNA-Seq data with or without a reference genome. BMC Bioinformatics 12:323. https://doi.org/10.1186/1471-2105-12-323

Lucini T, Panizzi AR (2017) Behavioral comparisons of ingestion and excretion by selected species of Pentatomids: evidence of feeding on different food sources supports pest status. Neotrop Entomol 46:361–367

Madeira F, Pearce M, Tivey AR, Basutkar P, Lee J, Edbali O et al (2022) Search and sequence analysis tools services from EMBL-EBI in 2022. Nucleic Acids Res 50:276–279

Mogilicherla K, Howell JL, Palli SR (2018) Improving RNAi in the brown Marmorated Stink Bug: identification of target genes and reference genes for RT-qPCR. Sci Rep 8:3720

Moraes MCB, Pareja M, Laumann RA, Borges M (2008) The chemical volatiles (semiochemicals) produced by neotropical stink bugs (Hemiptera: Pentatomidae). Neotrop Entomol 3:489–505

Nguyen LT, Schmidt HA, Von Haeseler A, Minh BQ (2014) IQ-TREE: a fast and effective stochastic algorithm for estimating maximum-likelihood phylogenies. Mol Biol Evol 32:268–274

Pal E, Allison JD, Hurley BP, Slippers B, Fourie G (2023) Life history traits of the Pentatomidae (Hemiptera) for the development of pest management tools. Forests 14:861

Panizzi AR (1987) Nutritional ecology of seed-suking insects of soybean and their management. Mem Inst Oswaldo Cruz 82:161–175

Panizzi AR (1997) Wild hosts of Pentatomids: ecological significance and role in their pest status on crops. Annu Rev Entomol 42:99–122

Panizzi AR, Lucini T, Aldrich JR (2022) Dynamics in pest status of phytophagous stink bugs in the Neotropics. Neotrop Entomol 51:18–31

Paula DP, Togawa RC, Costa MM, Grynberg P, Martins NF, Andow DA (2016) Identification and expression profile of odorant-binding proteins in *Halyomorpha halys* (Hemiptera: Pentatomidae). Insect Mol Biol 25(5):580–594

Pelosi P, Zhou JJ, Ban LP, Calvello M (2006) Soluble proteins in insect chemical communication. Cell Mol Life Sci 63:1658–1676

Pfaffl MW (2001) A new mathematical model for relative quantification in real-time RT–PCR. Nucleic Acids Res 29:e45

Rane RV, Ghodke AB, Hoffmann AA, Edwards OR, Walsh TK, Oakeshott JG (2019) Detoxifying enzyme complements and host use phenotypes in 160 insect species. Curr Opin Insect Sci 31:131–138

Rider DA, Schwertner CF, Vilímová J, Rédei D, Kment P, Thomas DB (2017) Higher systematics of the pentatomoidea. In: McPherson JE (ed) Invasive stink bugs and related species (Pentatomoidea): Biology, higher systematics, semiochemistry, and management. CRC Press, Boca Ratón, Florida, pp 25–201

Riga M, Denecke S, Livadaras I, Geibel S, Nauen R, Vontas J (2020) Development of efficient RNAi in *Nezara viridula* for use in insecticide target discovery. Arch Insect Biochem Physiol 103:e21650. https://doi.org/10.1002/arch.21650

Saha S, Allen KC, Mueller LA, Reddy GVP, Perera OP (2022) Chromosome length genome assembly of the redbanded stink bug, *Piezodorus guildinii* (Westwood). BMC Res Notes 15:115

Sánchez-Gracia A, Vieira F, Rozas J (2009) Molecular evolution of the major chemosensory gene families in insects. Heredity 103:208–216. https://doi.org/10.1038/hdy.2009.55

Schvartzman C, Fresia P, Murchio S, Mujica MV, Dalla-Rizza M (2022) RNAi in *Piezodorus guildinii* (Hemiptera: Pentatomidae): transcriptome assembly for the development of pest control strategies. Front Plant Sci 13:804839

Singh KS, Cordeiro EMG, Hunt BJ, Pandit AA, Soares PL, Correa A et al (2023) The genome sequence of the Neotropical brown stink bug, *Euschistus heros* provides insights into population structure, demographic history and signatures of adaptation. Insect Biochem Mol Biol 152:103890

Sosa-Gómez DR, Corrêa-Ferreira BS, Kraemer B, Pasini A, Husch PE, Vieira D et al (2020) Prevalence, damage, management and insecticide resistance of stink bug populations (Hemiptera: Pentatomidae) in commodity crops. Agr Forest Entomol 22:99–118

Sparks ME, Bansal R, Benoit JB, Blackburn MB, Chao H, Chen M et al (2020) Brown marmorated stink bug, *Halyomorpha halys* (Stål), genome: putative underpinnings of polyphagy, insecticide resistance potential and biology of a top worldwide pest. BMC Genom 21:227

Sparks M, Shelby K, Kuhar D, Gundersen-Rindal D (2014) Transcriptome of the invasive brown marmorated stink bug, *Halyomorpha halys* (Stal) (Heteroptera: Pentatomidae). PLoS ONE 9:e111646

Taiz L, Zeiger E (2004) Plant physiology, 3rd edn. Sinauer Associates Inc. Publishers, Sunderland, MA

Temple JH, Davis JA, Hardke J, Moore J, Leonard BR (2013) Susceptibility of southern green stink bug and redbanded stink bug to insecticides in soybean field experiments and laboratory bioassays. Southwest Entomol 38:393–406

Teufel F, Almagro Armenteros JJ, Johansen AR, Gíslason MH, Pihl SI, Tsirigos KD et al (2022) SignalP 60 predicts all five types of signal peptides using protein language models. Nature Biotech 40(7):1023–1025. https://doi.org/10.1038/s41587-021-01156-3

Vandesompele J, De Preter K, Pattyn F, Poppe B, Van Roy N, Paepe De et al (2002) Accurate normalization of real-time quantitative RT-PCR data by geometric averaging of multiple internal control genes. Genome Biol 3:1–11

Vogt RG (2003) Biochemical diversity of odor detection: OBPs ODEs and SNMPs. In: Blomquist GJ, Vogt RG (eds) Insect Pheromone Biochemistry and Molecular Biology. Elsevier Academic Press, London, pp 391–445

Volonté M, Traverso L, Estivalis JML, Almeida FC, Ons S (2022) Comparative analysis of detoxification-related gene superfamilies across five hemipteran species. BMC Genomics 23:757

Waterhouse AM, Procter JB, Martin DMA, Clamp M, Barton GJ (2009) Jalview version 2-A multiple sequence alignment editor and analysis workbench. Bioinformatics 25:1189–1191

Wu S, Deng W, Li M, Xiao Y, Li J, Teng K et al (2020) Analysis of chemosensory genes in full and hungry adults of *Arma chinensis* (Pentatomidae) through antennal transcriptome. Front Physiol 11:588291

Wu ZZ, Cui Y, Qu MQ, Lin JH, Chen MS, Bin SY, Lin JT (2019) Candidate genes coding for odorant binding proteins and chemosensory proteins identified from dissected antennae and mouthparts of the southern green stink bug *Nezara viridula*. Comp Biochem Physiol Part D Genomics Proteomics 31:100594. https://doi.org/10.1016/j.cbd.2019.100594

Xu C, Yong-Tao Li C, Tony Kong A-N (2005) Induction of phase I, II and III drug metabolism/transport by xenobiotics. Arch Pharmacol Res 28:249–268

Zhou JJ, Huang W, Zhang GA, Pickett JA, Field LM (2004) "Plus-C" odorant-binding protein genes in two *Drosophila* species and the malaria mosquito *Anopheles gambiae*. Gene 327:117–129. https://doi.org/10.1016/j.gene.2003.11.007